SSRG International Journal of Electrical and Electronics Engineering
ISSN: 2348-8379/ https://doi.org/10.14445/23488379/IJEEE-V13I5P107

Volume 13 Issue 5, 78-94, May 2026

Original Article

Simulation and Experimental Validation of DRL-PSO Empowered MPPT Approach for Partially Shaded PV System

Sanju[1], Kusum Lata Agarwal[2], Satya Sai Srikant[3], S Nallusamy[4]

[1]*Department of Electrical and Electronics Engineering, SRM Institute of Science and Technology, Delhi-NCR Campus, Modinagar, Ghaziabad, U.P., India.*
[2]*Karnavati University, Gandhinagar, Gujarat, India.*
[3]*Department of Electronics and Communication Engineering, SRM Institute of Science and Technology, Delhi-NCR Campus, Modinagar, Ghaziabad, U.P., India.*
[4]*School of Engineering Management and Continuing Education, Jadavpur University, Kolkata, India.*

[2]*Corresponding Author : kusum@karnavatiuniversity.edu*

Received: 12 February 2026 Revised: 11 March 2026 Accepted: 10 April 2026 Published: 30 May 2026

Abstract - *Harvesting the maximum available power from a solar Photovoltaic (PV) installation is one of the most critical control challenges, particularly when the environment offers fluctuating irradiance together with partial shading on the array. To deal with this issue, the present manuscript brings forward a novel hybrid Maximum Power Point Tracking (MPPT) scheme in which a Deep Reinforcement Learning (DRL) module, built around the Deep Deterministic Policy Gradient (DDPG) algorithm, has been integrated with Particle Swarm Optimisation (PSO). An embedded artificial-intelligence agent has been further incorporated so that the controller can adapt itself in real time to the prevailing conditions. The actual irradiance and ambient temperature recorded on 20 June 2025 at Ghaziabad city (28.6692° N, 77.4538° E) in northern India have been used as the validation profile. The proposed scheme has been implemented in a LabVIEW environment. Its behaviour has been benchmarked against four well-established techniques, namely Perturb & Observe, Fuzzy Logic, Artificial Neural Network (ANN), and Model Reference Adaptive Control (MRAC), considering parameters such as settling time, voltage and current fluctuations, transient response, and behaviour under shaded operation. The recorded results bring out a tracking efficiency of 99.79 percent against 96.87 percent (P&O), 98.50 percent (Fuzzy), 98.84 percent (ANN), and 99.76 percent (MRAC). The settling interval has been measured at nearly 2.6 ms. At the same time, the voltage and current ripples have been confined to 0.029 V and 0.025 A, with Root Mean Square Error (RMSE), Mean Absolute Error (MAE), and Mean Absolute Percentage Error (MAPE) values of 0.00187, 0.00191, and 0.22 percent, respectively.*

Keywords - *AI Agent, Maximum Power Point Tracking, Partial Shading, Deep Reinforcement Learning, PSO Optimization*

1. Introduction

Out of the various renewable sources, solar Photovoltaic (PV) generation has witnessed an unprecedented expansion in recent years. The International Energy Agency (IEA) anticipates that global energy consumption will increase by almost 50% by 2050, indicating that the world's energy environment is rapidly changing [1]. The cumulative installed PV capacity across the globe crossed one Terawatt (TW) during 2023 and is projected to double by the year 2030. This rapid growth has been driven mainly by an 85% reduction in module prices since 2010, along with significant advancements in cell technology [IEA PVPS, 2024]. Despite such promising progress, PV systems continue to suffer from several practical limitations that restrict the realisation of their full energy harvesting potential. On Standard Test Condition (STC) of an irradiance of 1000 W/m² and cell temperature of 25°C, the typical conversion efficiency of commercial modules remains confined within 15% to 22%. In real-field deployment, this efficiency is further reduced due to dust accumulation, shading, temperature rise, and other environmental disturbances. The non-linear behaviour of the PV current–voltage curve is the principal reason behind these losses, since the operating point shifts continuously amidst fluctuating irradiance and temperature.

In the absence of an efficient tracking mechanism, the operating point of the PV array drifts away from its true maximum power point, and the annual energy yield falls by nearly 15 to 40 percent [2]. This loss is even more severe when the array is exposed to partial shading, where the power–

voltage curve exhibits multiple local peaks and a single global peak. To recover the maximum possible energy from such a non-linear and time-varying source, a dedicated MPPT algorithm is, therefore, essential. [3] The primary research gap is that traditional MPPT approaches, like Perturb & Observe (P&O) and Incremental Conductance (InC), are unable to make the distinction between local and global maxima. At the same time, pure metaheuristic methods such as PSO, Grey Wolf Optimization (GWO), or Salp Swarm Optimisation (SSO) suffer from premature convergence and high steady-state oscillations. On the other hand, learning-based controllers like ANN or fuzzy logic require offline training and lose adaptability when the operating environment changes rapidly. A unified framework that simultaneously offers fast global search, online adaptation, low ripple, and reduced convergence time under both uniform and non-uniform conditions is still missing in the published literature. The present work has been formulated to address exactly this gap.

Motivated by the above-mentioned gap, the present study introduces a hybrid MPPT controller in which PSO is intelligently fused with a Deep Deterministic Policy Gradient (DDPG) based DRL agent. The novelty of the proposed scheme lies in three aspects. First, an adaptive weighting law is formulated, which automatically transfers control authority to PSO during slow and uniform irradiance changes and shifts it to the DDPG agent during sudden disturbances or partial shading, thereby exploiting the strengths of both methods within a single control loop. Second, the entire framework has been validated on real-time irradiance and temperature data recorded at Ghaziabad, India (28.6692° N, 77.4538° E) on 20 June 2025, which adds geographical relevance to the Indian climatic context that is rarely reported in earlier studies. Third, a lightweight AI agent has been embedded in the controller for online tuning and supervisory monitoring through MQTT and HTTP protocols. The proposed controller achieves a tracking efficiency of 99.79%, a convergence time of 2.6 ms, and voltage and current ripples of 0.029V & 0.025A, respectively, which are demonstrably superior to the values reported. [9, 11, 13, 17] The remainder of the manuscript has been structured as follows. Section 2 provides the literature survey, Section 3 explains the PV uncertainty model, Section 4 describes the boost converter, Section 5 presents the proposed DRL–PSO controller, Section 6 discusses simulation and hardware results, and Section 7 summarises the conclusions along with future work.

2. Literature Review

Numerous MPPT techniques have been documented in literature over the last 20 years, broadly categorised into conventional, soft-computing, and metaheuristic approaches. The conventional family, which includes P&O and InC, gained early popularity owing to its simple structure and limited sensor requirement. Under uniform irradiance, these methods can deliver tracking efficiency of around 95–98 percent. [4] However, when the array is subjected to Partial Shading Conditions (PSCs), the power–voltage curve develops a single global peak along with several local maxima. In such situations, the gradient-based logic of P&O and InC frequently locks the operating point at a local peak, and a substantial portion of the available power is lost. [5-7] To overcome this fundamental shortcoming, researchers have progressively shifted towards metaheuristic and learning-based optimisation techniques.

A current-sensor-based MPPT controller using sequential golden section search has been developed for an isolated DC microgrid where only one sensor was sufficient to track the MPP, thereby reducing the cost of instrumentation. [8] Building further on swarm intelligence, the authors applied the SSO algorithm to a hybrid PV-thermoelectric generator working under PSCs and non-uniform thermal distribution. [9] Their experimental observations indicated that SSO could damp the power oscillations effectively and yielded a tracking efficiency of over 99 percent.

The Arithmetic Optimisation Algorithm (AOA) was applied for PV-fed battery charging systems operating under PSCs, and the work reported reduced settling time as compared to PSO. [10] The investigation put forward a two-stage MPPT scheme in which an improved Artificial Bee Colony (ABC) optimiser was integrated with the Simultaneous Heat Transfer Search (SHTS) method. [11] Such a combination was found capable of locating the global MPP even in the presence of multiple peaks. The authors introduced a Grey-Wolf-based Robust Unified Control Algorithm intended for grid-connected PV systems and demonstrated improved disturbance rejection. [12]

A Modified Coot Optimisation Algorithm (MCOA) was put forward in order to address the difficulty of tracking the global MPP under fast-varying weather conditions. [13] The reported results revealed an average tracking time of nearly 1.3 seconds along with a tracking efficiency close to 99.87 percent across the test scenarios.

An interharmonic mitigation method was developed for single-phase grid-connected PV systems. [14] The authors blended the Genetic Algorithm (GA) with the Fractional Open Circuit Voltage (FOCV) method to form a hybrid MPPT controller, which was tested in MATLAB/Simulink under both uniform and non-uniform irradiance profiles. [15]

The comparative study examined Adaptive Neuro-Fuzzy Inference System (ANFIS) along with P&O, InC, GN, PSO, and Fuzzy Logic Controller (FLC), and concluded that ANFIS produced a faster transient response while the remaining algorithms were better suited to dynamic operating conditions. [16] The authors explored a hybrid DRL–PSO formulation to improve the performance of a solar PV module. [17] The authors reviewed the use of bypass diodes in mitigating shading effects and hotspot formation. [18, 19] The

investigation reported in [20] discussed a Modified SSA for solar PV applications. More recently, DRL has emerged as a promising direction for self-learning MPPT controllers. The DDPG-based controller proposed in [24] showed improved adaptability under varying irradiance, while a hybrid GWO–DDPG scheme reported in [25] was found to deliver lower steady-state ripple. A review of artificial intelligence-based MPPT methods presented in further confirmed that data-driven controllers can outperform classical metaheuristics, provided that the training and exploration mechanisms are designed carefully.

2.1. Research Gaps

A careful examination of the above literature reveals that, in spite of considerable progress, several gaps still exist in the present generation of MPPT controllers. Conventional methods such as P&O and InC are reported to display rather slow response times of the order of more than 40 ms, together with efficiency below 97 percent under PSCs. Although metaheuristic algorithms such as SSA and AOA can attain efficiency values of more than 99 percent, their performance has been observed to depend strongly on user-defined parameter tuning, and they are, therefore, not well-suited for environments that experience rapid disturbances. [21] Moreover, the existing hybrid DRL–PSO scheme was validated only through MATLAB simulation, and a quantitative comparison against MRAC, ANN, or fuzzy controllers under real-time recorded irradiance was not provided. [17] Existing studies have not reported convergence times below 1 ms, which is essential for fast-changing irradiance profiles encountered in tropical regions such as the northern Indian climate. [9, 11, 13]

AI-based controllers like fuzzy logic and ANFIS have shown improved adaptability, yet they require offline training data, and their inference logic is fixed once deployed. [22] As a consequence, most of the existing MPPT solutions are unable to address the combined challenge of (i) high uncertainty in irradiance and temperature, (ii) operational degradation of the PV cells with time, and (iii) modelling inaccuracies in the boost converter dynamics. There is, therefore, a detailed research need for a unified controller that combines the global search capability of a metaheuristic technique with the online learning capability of a DRL agent, supported by a real-time supervisory module. The proposed DRL–PSO controller addresses each of these gaps, and the achieved improvement over [9, 11, 13, 17] is established quantitatively in Section 6.

3. Uncertainty in Solar PV System and Modeling

The performance of a solar photovoltaic installation is influenced by a number of uncertain factors, both environmental and operational, which together govern the actual energy yield. To enable an accurate MPPT strategy under such uncertainty, suitable mathematical models that capture the non-linear cell behaviour are essential. Earlier studies have indicated that, when these uncertainties are not addressed by an appropriate controller, the annual energy generation can drop by nearly 20 to 50 percent [23]. The presence of PSCs further worsens the situation as the irradiance distribution across the array becomes uneven, leading to forced activation of bypass diodes and the development of localised hot spots within the affected modules.

3.1. PV System Modelling

For analytical and simulation purposes, the photovoltaic cell has been represented through the standard single-diode equivalent circuit, which is presented in Figure 1. Within this representation, the cell is taken as a current source generating Photocurrent (I_{ph}) connected across a diode together with a Parallel Shunt Resistance (R_{sh}), and this combination has been placed in series with the Loss Resistance (R_s).

The net terminal current (I) supplied by the cell can therefore be expressed as:

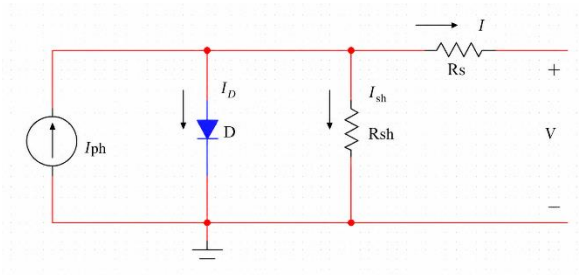

Fig. 1 Equivalent Circuit Diagram Of The One-Diode Pv Cell Model

$$I = I_{ph} - I_D - I_{sh} \quad (1)$$

$$I = I_{ph} - I_o\left(exp\left(\frac{q(V+IR_s)}{akT}\right) - 1\right) - \left(\frac{V+IR_s}{R_{sh}}\right) \quad (2)$$

The Photocurrent (I_{ph}) is a function of the prevailing Solar Irradiance Level (G) as well as the operating cell Temperature (T), and may be obtained as

$$I_{ph} = \frac{G}{G_{ref}}\left[I_{sc} + \alpha_1\left(T - T_{ref}\right)\right] \quad (3)$$

where G_{ref} = 1000 W/m^2, T_{ref} = 298K, I_{sc} is the short-circuit current, and α_1 is the current temperature coefficient. The parameters used for the simulation of the one-diode model are depicted in Table 1.

The diode reverse saturation current I_o can be expressed in the following form:

$$I_o = \frac{I_{sc}}{exp\left(\frac{q\,V_{oc}}{akT}\right)-1} \quad (4)$$

The single-diode equation set discussed above has been built up inside the LabVIEW environment, and the corresponding block-diagram realisation appears in Figure 2. At every sampling instant, the model receives the live irradiance and temperature readings and computes the resulting PV terminal output.

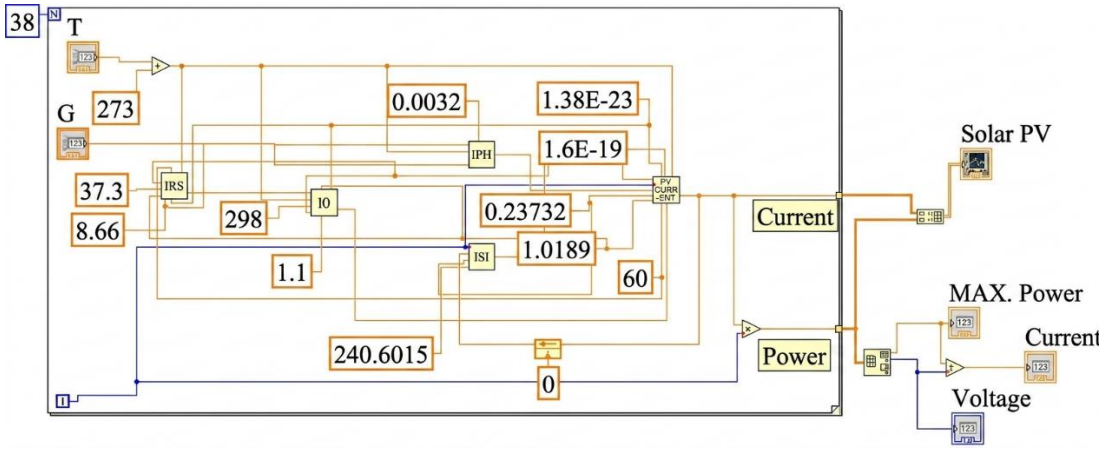

Fig. 2 LabVIEW block diagram of the one-diode PV model

Table 1. Parameters utilized in the one-diode model simulation

Parameter	Short circuit current	Open circuit voltage	Ideality factor	Series resistance	Shunt resistance	Current temperature coefficient	Voltage temperature coefficient
Symbol	I_{sc}	V_{oc}	a	R_s	R_{sh}	α_1	β_V
Value	8.21	37	1.3	0.22	415	0.004	-0
Unit	A	V	-	Ω	Ω	/°C	/°C

3.2. I-V and P-V Characteristics

The current–voltage and power–voltage profiles of the considered PV module, captured on STC, are jointly plotted in Figure 3. From the graph, it can be seen that the maximum power point lies near a terminal voltage of about 31 V, together with a current close to 7.98 A, which yields a peak generation of nearly 247.3 W.

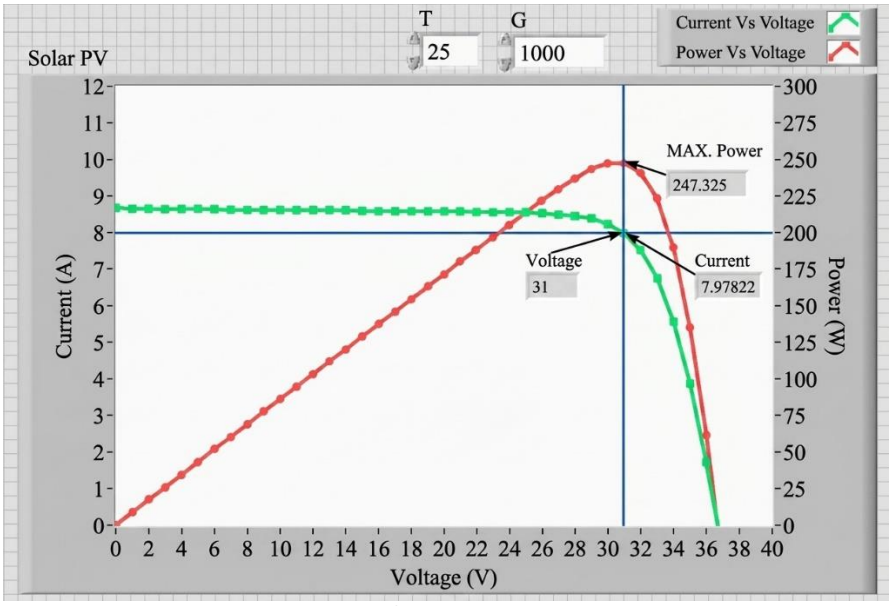

Fig. 3 I-V and P-V profiles under STC, highlighting MPP

3.3. PV module under PSCs

In a practical rooftop or field installation, partial shading is encountered very frequently and is mainly produced by moving clouds, neighbouring structures, or surrounding vegetation. Whenever only a portion of a module receives full sunlight while the remaining portion remains shaded, the overall electrical behaviour of the array deviates significantly from its ideal pattern. To bring this effect into focus, a 60-cell PV module has been segmented into three groups within the simulation set-up of Figure 4, with each group subjected to a different combination of irradiance and temperature. The first 20 cells are kept at 1000 W/m² and 25 °C, the next 20 cells (numbered 21 to 40) at 700 W/m² and 24.5 °C, and the last group of 20 cells (numbered 41 to 60) at 400 W/m² and 24 °C.

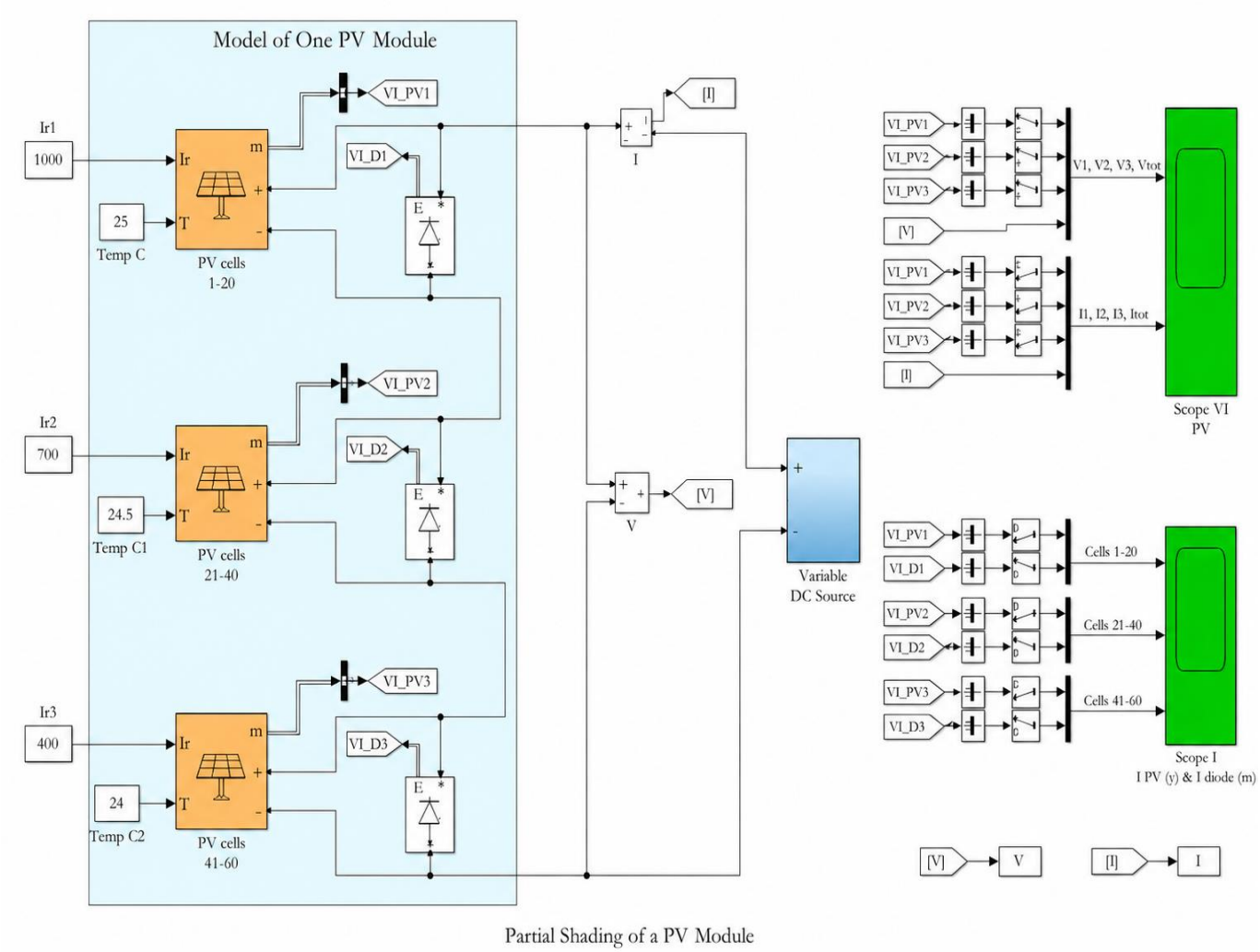

Fig. 4 Simulation model of PV module under partial shading

For such an unevenly illuminated arrangement, the I–V trace is no longer obtained as a single smooth curve, as is the case under uniform irradiance, and the resulting profile of Figure 5 carries a number of step-like discontinuities. Every such discontinuity marks the moment at which a particular group of cells, no longer able to support the prevailing string current, gets short-circuited through its bypass diode, resulting in a sudden fall of current at the corresponding voltage point.

A side-by-side comparison of conventional MPPT algorithms with the proposed method, depicted in Figure 6, brings out the strength of the DRL–PSO scheme. Whereas the conventional methods are seen to settle on a sub-optimum local maximum, the DRL–PSO scheme is observed to consistently identify the genuine global peak. The simulation outcomes confirm that the proposed approach delivers higher output power along with efficiency above 99 percent, while P&O is sometimes seen to fall below 97 percent. The same complexity is also reflected in the corresponding P–V curve plotted in Figure 6, where multiple local crests appear in addition to the true global maximum. If the controller mistakenly converges on any of these local peaks rather than the global one, a considerable share of the available solar energy is lost.

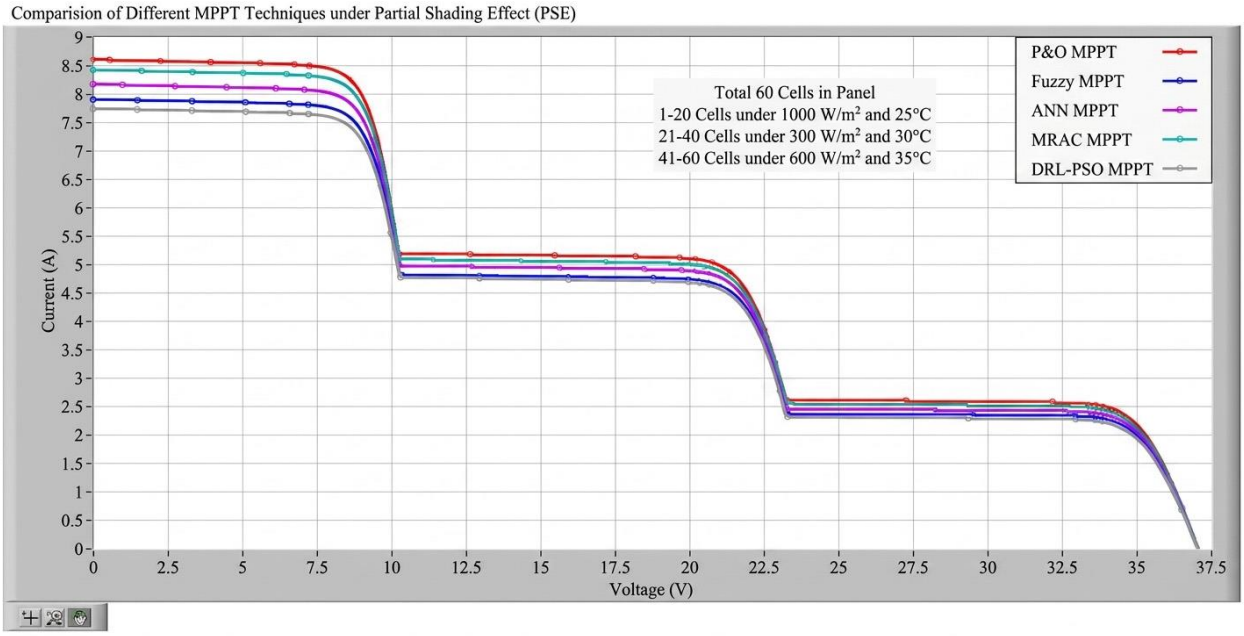

Fig. 5 I–V characteristics under partial shading, comparing different MPPT techniques

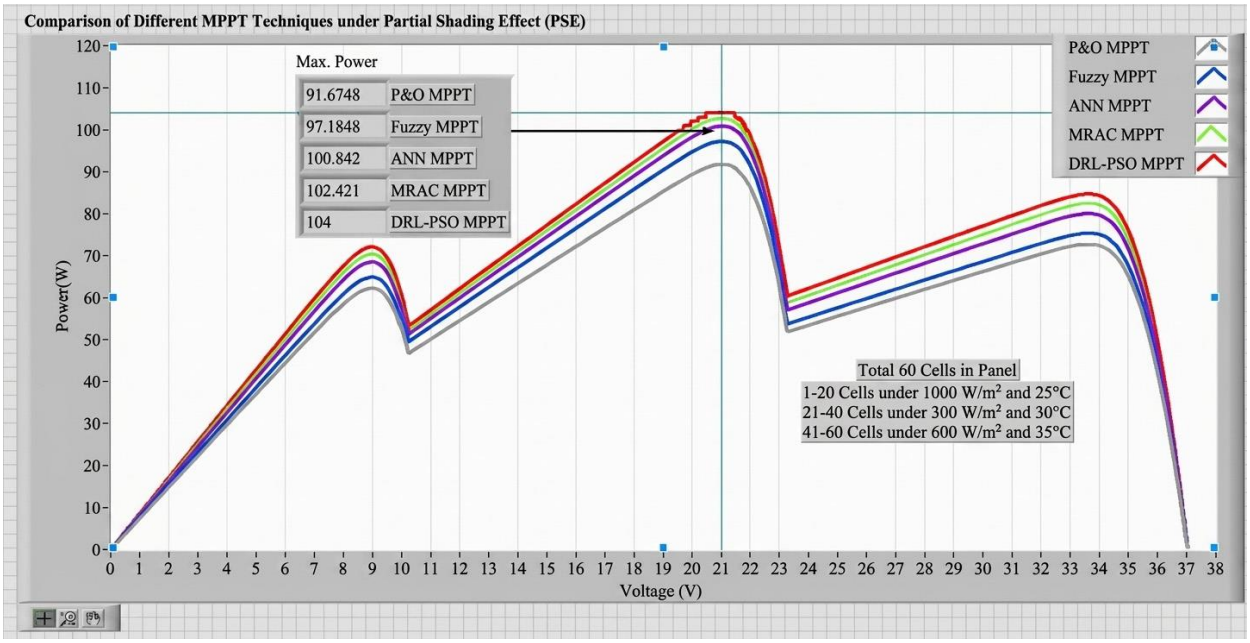

Fig. 6 P–V characteristics under partial shading

4. Boost Converter Model

Within a typical PV power conditioning chain, a DC–DC boost converter acts as the key interfacing stage between the solar generator and the connected load.

The two principal roles played by this converter are firstly to step up the array output voltage so that it can satisfy the DC-bus or load voltage requirement, and secondly to enable MPPT by varying the Duty Cycle (D) of the switching pulse in a closed-loop manner.

4.1. Topology and Steady-State Operation

As shown in Figure 7, the considered boost stage is built up from an energy-storage inductor *L*, a controlled switch (MOSFET), a freewheeling diode, an output filtering capacitor *C*, and load *R* together with the load resistance, as is depicted in Figure 7.

The proposed MPPT block continuously samples the PV terminal voltage V_{pv} and current I_{pv}, and adjusts the duty ratio D ($0 < D < 1$) in order to drive the array towards its MPP.

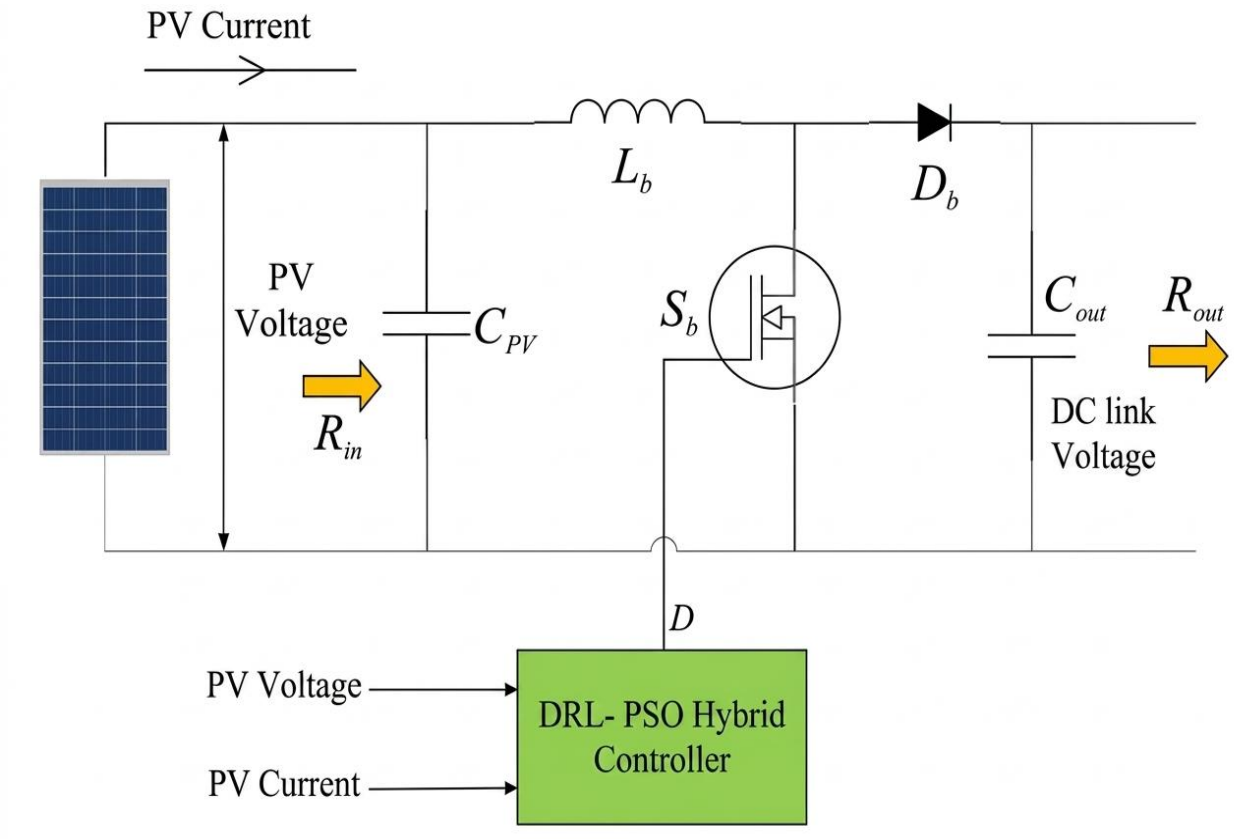

Fig. 7 Schematic diagram of PV system with MPPT and DC–DC boost converter

For an idealised continuous-conduction operation in steady state, the input-to-output voltage relation, where the input voltage is denoted as V_{in} and the output voltage V_{out} of the boost converter is given by:

$$\frac{V_o}{V_{in}} = \frac{1}{1-D} \tag{5}$$

$$\Delta I_L = \frac{V_{in} \times D}{L \times f_{sw}} \tag{6}$$

Where f_{sw} denotes the operating switching frequency of the converter.

4.2. Small-Signal Dynamic Model

In order to study and tune the transient behaviour of the boost stage – particularly its response to abrupt changes in irradiance or in the connected load – a linearised small-signal representation of the converter has been employed in the present work.

The procedure consists of perturbing the non-linear averaged model around its DC operating point so that the resulting set of equations can be analysed in the frequency domain.

If the small perturbations in the terminal voltage, terminal current, and duty ratio are taken as $\tilde{v}$, $\tilde{\imath}$, and $\tilde{D}$ In that order, then in the immediate vicinity of the MPP, the PV array can be modelled as an equivalent dynamic resistance. (R_{pv}) whose value is governed by the local slope of the I–V curve at that operating point.

The averaged converter equations are obtained by integrating the switching-period dynamics, after which a linearisation is performed about the DC operating point. The transfer function that links the perturbation in the duty ratio $(\tilde{D})$ to changes in output voltage $(\tilde{v}_{out})$ can be obtained (assuming no battery dynamics for simplicity):

$$\frac{\tilde{V}_{out}(s)}{\tilde{D}(s)} = G_{vd}(s) \tag{7}$$

where $G_{vd}(s)$ is the voltage-to-duty cycle transfer function in the Laplace domain, and s is the complex frequency variable.

5. Proposed DRL-PSO-based MPPT controller

The MPPT scheme proposed in the present work has been formulated by integrating the swarm-based exploration capability of PSO with the policy-learning ability of the

DDPG variant of deep reinforcement learning. By such an integration, the limitations associated with both conventional and stand-alone advanced MPPT controllers, particularly when the system has to operate under quickly varying weather and partial-shading conditions, can be effectively overcome.

Within this hybrid framework, the PSO unit takes care of a fast population-based exploration and quickly narrows the search to the promising region on the P–V curve, while the DRL unit, through online policy refinement, is responsible for fine-tuning and locking the operating point exactly at the true global MPP.

A novel adaptive weighting law has additionally been introduced so that a smooth balance between exploration and exploitation can be maintained at every operating instant.

The complete algorithm has been verified both in simulation and on a real hardware test-bench built around LabVIEW with NI-DAQ, and dependable tracking has been observed even under intense shading and abruptly changing irradiance.

5.1. Objective Function and Adaptive Blending

The resultant duty ratio D_{final} obtained at every step is therefore an adaptive linear combination of the DRL output D_{DRL} and PSO D_{PSO} together with the PSO output, where the contribution of each branch is governed by a weighting parameter, λ:

$$D_{final} = \lambda . D_{DRL} + (1 - \lambda) . D_{PSO} \quad (8)$$

$$v_{i,k+1} = w . v_{i,k} + c_1 . rand_1 . (pbest_i - x_{i,k}) + c_2 . rand_2 . (gbest - x_{i,k}) \quad (9)$$

where w represents the inertia coefficient, while c_1, c_2 denote the cognitive and social acceleration factors, and $rand_1$, $rand_2$ are uniformly distributed random numbers between 0 and 1.

While the PSO loop provides rapid convergence under steady irradiance, it has a known tendency to get stuck in local optima during shading, which is precisely why the present work hybridizes it with the DRL agent.

5.2. Deep Reinforcement Learning (DRL) control agent

In the present formulation, the MPPT problem has been recast as a continuous-action Markov Decision Process and solved using the DDPG framework.

The state vector $s_t$is built from the real-time PV measurements, such as the terminal voltage, the array current, and the cell temperature, while the action a_t corresponds to the incremental adjustment in the duty ratio. Internally, the DDPG framework relies on a pair of neural networks – an actor network that learns a deterministic state-to-action mapping and a critic network that approximates the action–value function. To stabilise the learning process and to obtain a smoother convergence, both of these networks are accompanied by their own target networks whose weights are updated only at a slow rate.

Among the tunable hyperparameters that have been considered in the present implementation are the learning rates of the actor and critic, the size of the experience replay memory, the mini-batch size used during training, and the parameters governing the Ornstein–Uhlenbeck noise process, which is employed for generating temporally correlated exploration signals.

5.3. Hybrid DRL-PSO Duty Cycle Controller

In the proposed hybrid scheme, the population-based exploration provided by PSO and the policy-driven fine-tuning offered by DDPG are dynamically merged through a single adaptive weighting parameter, λ.

The final duty cycle (d_{hybrid}) is constructed as a convex combination of the duty-ratio outputs produced individually by the DRL agent and the PSO loop:

$$d_{hybrid} = \lambda . d_{PSO} + (1 - \lambda) . d_{DRL} \quad (10)$$

The blending parameter λ is updated online as a function of the prevailing system dynamics, in the manner shown below:

$$\lambda = \lambda_o + k_\lambda . |\Delta P| \quad (11)$$

where λ_o is the base weight, k_λ is an empirically determined tuning coefficient, and $|\Delta P|$ represents the magnitude of the instantaneous power oscillation.

5.4. MPPT Control Loop

The MPPT control loop developed here works as a closed-loop optimisation engine that continuously drives the PV system towards the global maximum power point.

At every sampling interval, the present system states are first acquired from the boost converter and the array, after which the DRL and PSO branches independently propose a candidate duty ratio.

A blending stage then merges the two candidates as per the adaptive λ law and forwards the final duty ratio to the gate driver of the converter. The resulting array power is subsequently fed back so that both the DDPG policy and the PSO swarm can be progressively refined.

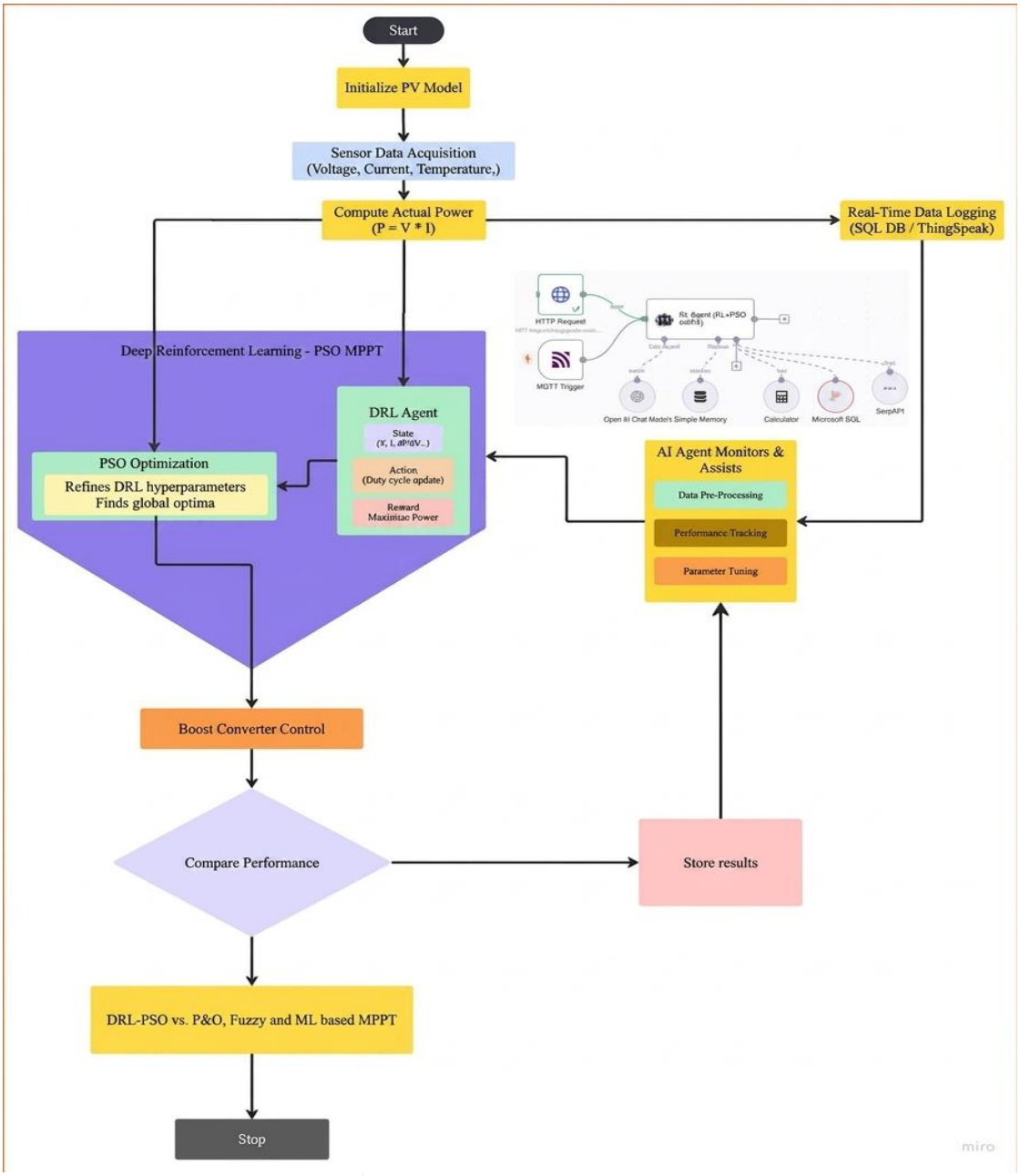

Fig. 8 Flowchart of the proposed hybrid DRL-PSO MPPT control system

- Measure PV voltage, current, and temperature.
- Generate a duty-cycle candidate from the DRL controller.
- Generate another duty-cycle candidate using PSO based on swarm search and best solutions.
- Blend both candidates using a dynamic weighting factor according to operating conditions.
- Apply the selected duty cycle to the DC–DC boost converter to drive the PV array toward MPP.
- Measure output power and use it as feedback to update the DRL policy and PSO best positions.
- Log data and monitor system performance through a supervisory module (see flowchart in Figure 8).

5.5. AI Agent Implementation and Real-Time Monitoring

To enhance the real-time response of the proposed DRL–PSO MPPT controller, an artificial-intelligence supervisory agent has been incorporated, as shown in Figure 9. The agent acquires the live operating measurements (irradiance, ambient and cell temperature, and the PV output power) through HTTP and MQTT communication channels in a continuous manner. By drawing on the embedded DDPG model, the agent carries out online inference and delivers refined duty-ratio commands to the converter. In parallel, the PSO routine is invoked at periodic intervals to re-optimise the controller hyperparameters with respect to the current performance

indices. The complete end-to-end loop has been measured to operate with a latency of less than 50 ms, while delivering nearly a 20 percent reduction in RMSE in comparison with non-AI controllers.

A local fallback module has been provided so that the controller can continue to function safely whenever the external communication links go down, which highlights the overall robustness of the implementation.

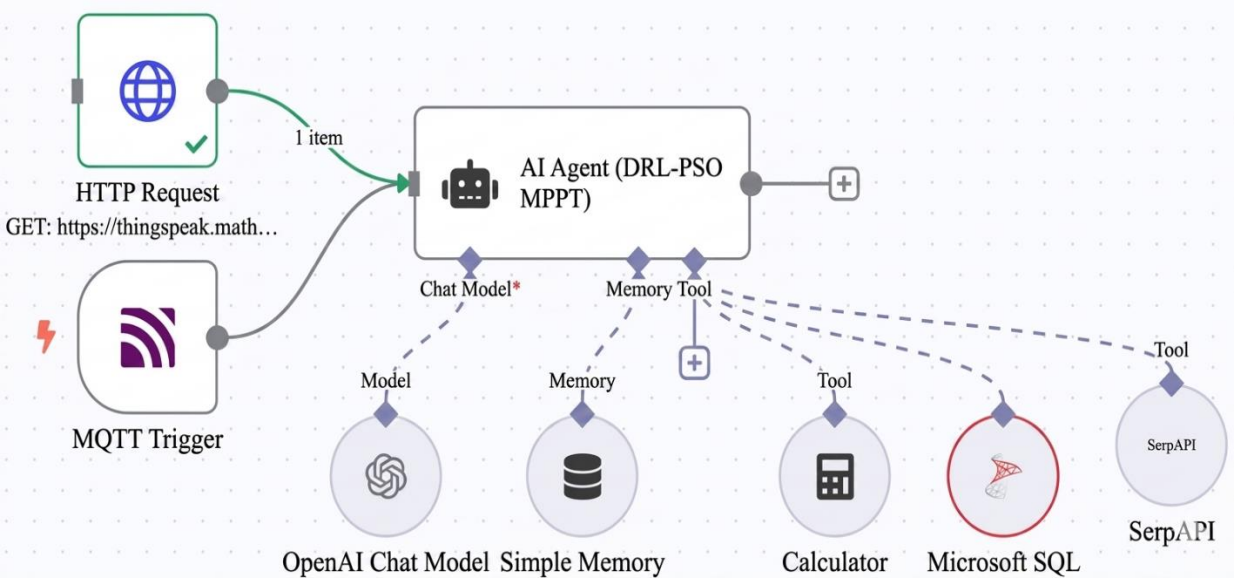

Fig. 9 Real-time data processing and AI agent architecture in DRL-PSO MPPT controller

6. Results and Discussions

The performance of the proposed DRL–PSO MPPT controller was thoroughly evaluated through both simulation in the LabVIEW environment and real-time hardware verification using a National Instruments (NI) DAQ system. The actual irradiance and temperature profile recorded on 20 June 2025 at Ghaziabad city (28.6692° N, 77.4538° E), together with sensor readings collected from the local meteorological setup, was used as the input data for the study, as shown in Figure 10.The recorded irradiance curve clearly captured the influence of transient cloud cover, with values fluctuating between nearly 70 W/m² in the early hours and a peak close to 1000 W/m² around solar noon, after which it gradually declined during the afternoon. The cell temperature was found to rise from about 30 °C in the early morning to more than 42 °C in the mid-day period, with a daily average of 35.2 °C. In order to systematically assess the controller, five distinct environmental test states were defined, and these are summarised in Table 2.

Following the operating profile of Figure 10, the proposed controller has been benchmarked against four established MPPT strategies, namely P&O, FLC, ANN controller, and MRAC. The benchmarking has been carried out under both steady irradiance and dynamically varying conditions, including the case of partial shading.

For State 1 corresponding to STC, the proposed DRL–PSO controller was found to converge to the MPP in a very short interval. As may be seen from Figure 11, the output power settled near 250 W in nearly 3.2 ms with an overshoot of less than 0.1 percent. The voltage ripple stayed below 0.07 V while the current ripple was limited to 0.038 A, both of which indicate excellent steady-state behaviour.

Within this hybrid arrangement, the PSO module is responsible for a quick population-based global search towards the MPP region, whereas the DDPG agent fine-tunes the duty cycle so that any residual oscillations get suppressed. In comparison, the traditional P&O technique displayed pronounced steady-state oscillations, with voltage and current ripples of nearly 4.07 V and 1.11 A, respectively, together with an overshoot of about 5 percent. The output of P&O eventually settled at 243 W, which corresponds to an efficiency of 97.47 percent.

The FLC and ANN-based controllers were observed to attenuate the ripples compared to P&O; a longer settling duration of nearly 20–30 ms was needed to reach the MPP. The MRAC controller delivered efficiency and ripple values close to those of the DRL-PSO scheme, but it lacks the dynamic exploration-exploitation balance that becomes critical whenever the irradiance changes abruptly.

Figure 13 illustrates that, among all the algorithms considered, the proposed DRL–PSO hybrid achieves the quickest and most accurate tracking of the MPP, with the smallest overshoot and ripple.

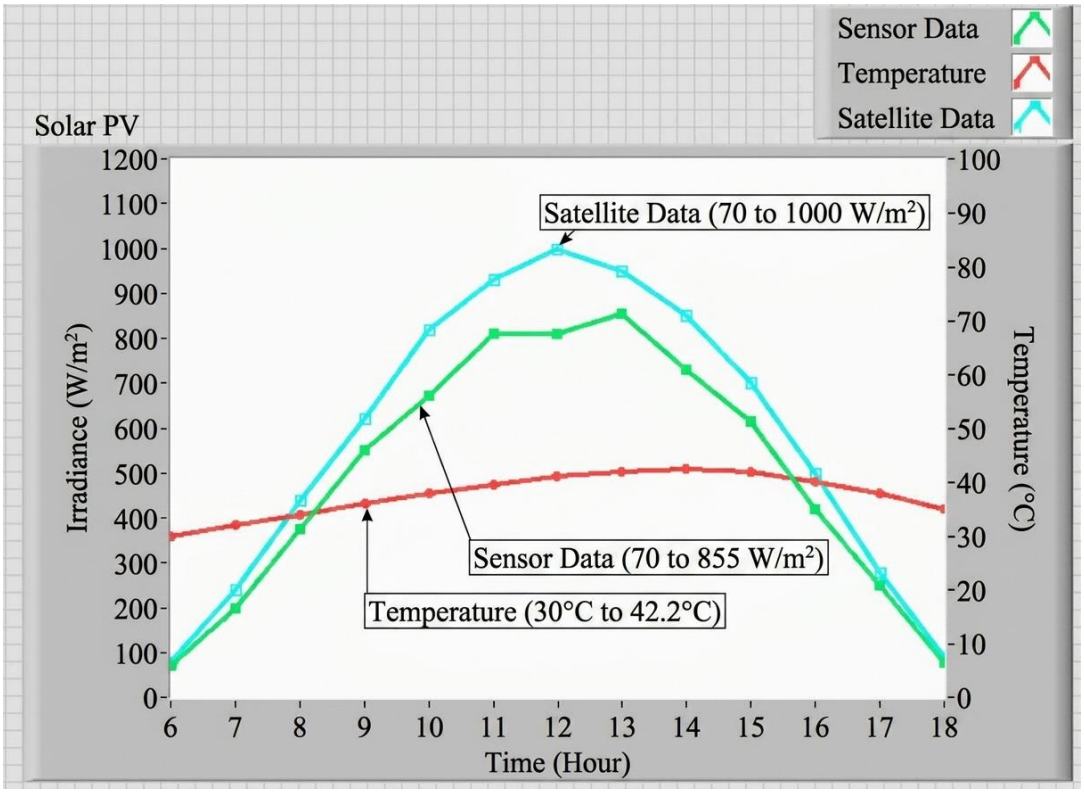

Fig. 10 Solar irradiance and temperature data for Ghaziabad City

Table 2. Environmental test states used for the performance evaluation of the MPPT controller

State	Irradiance (W/m²)	Temp. (°C)	Description
State 1	1000	25	STC
State 2	800	30	Moderate irradiance
State 3	600	35	Transitional condition
State 4	400	40	Low irradiance
State 5	200	45	Extreme low irradiance

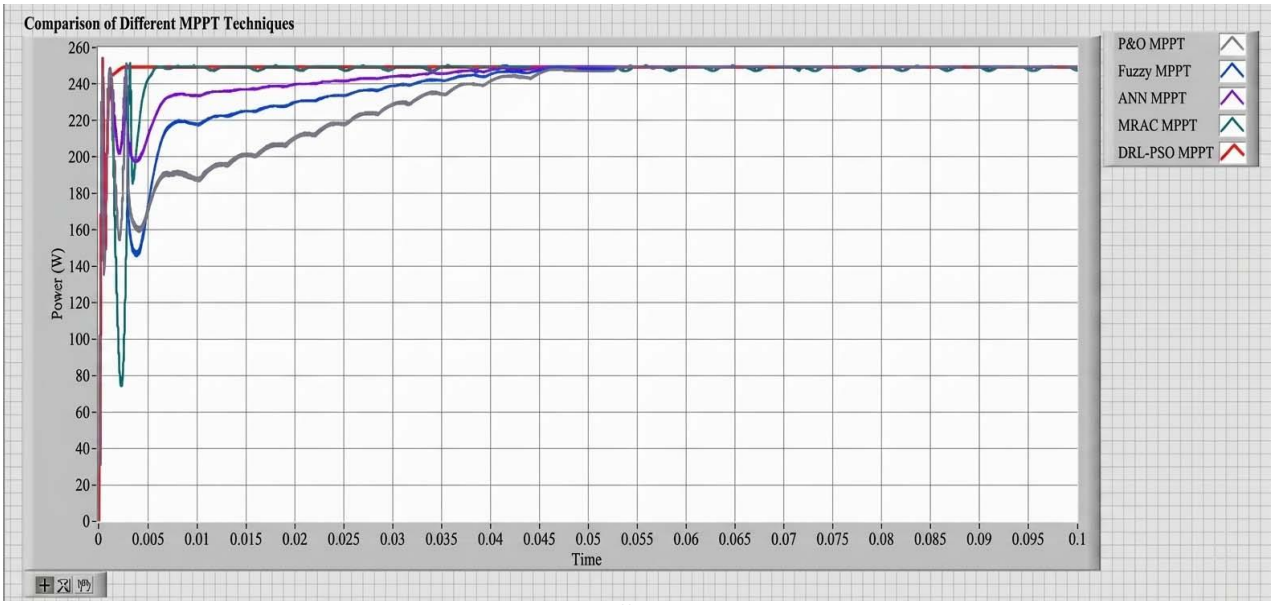

Fig. 11 The Pv power utilizing different MPPT techniques under STC

Figure 12 makes it visually evident that the proposed DRL–PSO hybrid arrives at the maximum-power point in the shortest interval and with the smallest residual oscillation when set side by side with the remaining controllers.

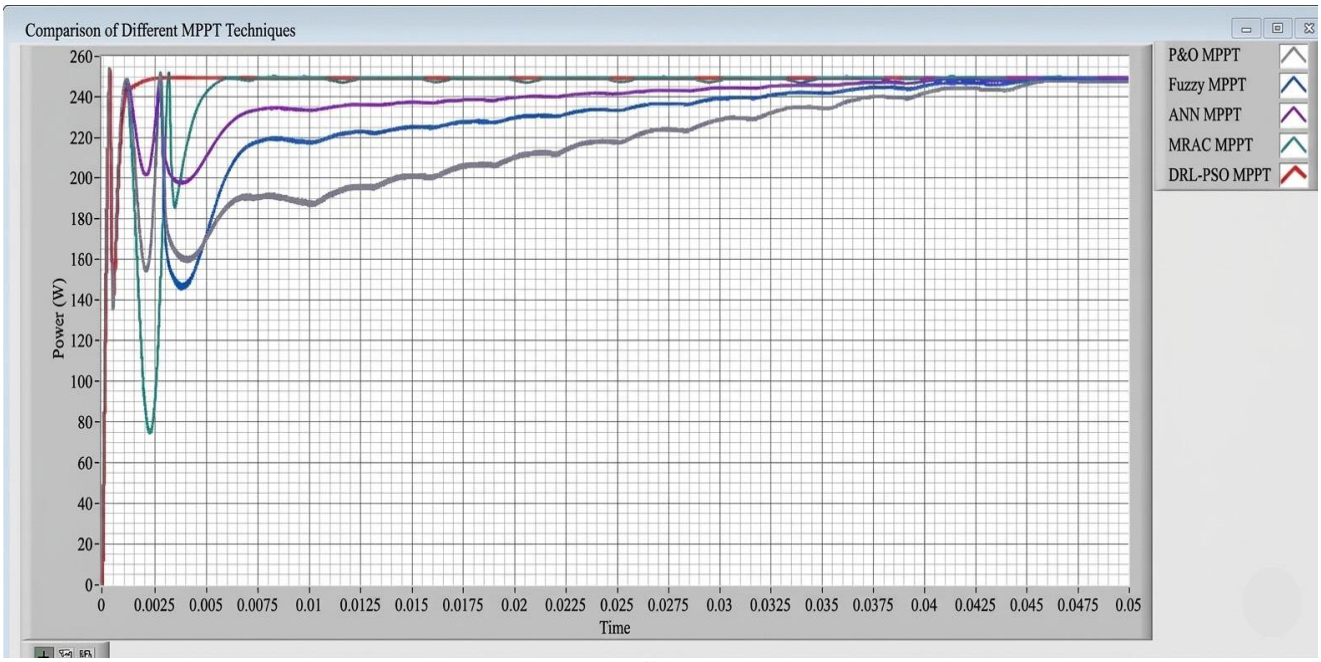

Fig. 12 The PV output power using different MPPT controllers (Scale 0 to 0.05)

From the entries of Table 3, it may be noted that the P&O technique exhibits the largest voltage and current ripples together with the lowest efficiency, especially when the operating conditions deviate from the ideal. The Fuzzy logic and ANN controllers do show an improvement over P&O, but they still suffer from a higher level of oscillation and a slower response than the proposed DRL–PSO scheme. While the MRAC controller offers a comparable performance under uniform irradiance, the DRL–PSO controller maintains its lead consistently in both dynamic and partially shaded scenarios on account of its adaptive hybrid mechanism. The corresponding performance indices for all the controllers are summarised in Table 4.

Table 3. Performance parameters of MPPT techniques across different states

Performance Parameters	MPPT Technique	State 1 (1000 W/m²,25 ° C)	State 2 (800 W/m²,30 ° C)	State 3 (600 W/m²,35 ° C)	State 4 (400 W/m²,40 ° C)	State 5 (200 W/m²,45 ° C)
Voltage ripple (V)	P&O	4.07 V	3.88 V	1.49 V	4.10 V	4.82 V
	Fuzzy	0.5 V	0.4 V	0.1 V	0.4 V	0.5 V
	ANN	0.3 V	0.2 V	0.05 V	0.2 V	0.3 V
	MRAC	0.08 V	0.04 V	0.03 V	0.01 V	0.02 V
	DRL-PSO	0.07 V	0.038 V	0.027 V	0.009 V	0.019 V
Current ripple (A)	P&O	1.11 A	1.15 A	0.48 A	1.03 A	0.10 A
	Fuzzy	0.3 A	0.3 A	0.1 A	0.2 A	0.05 A
	ANN	0.2 A	0.2 A	0.05 A	0.1 A	0.02 A
	MRAC	0.04 A	0.03 A	0.046 A	0.03 A	0.02 A
	DRL-PSO	0.038 A	0.028 A	0.03 A	0.02 A	0.01 A

Convergence time (s)	P&O	0.049 s	0.041 s	0.042 s	0.041 s	0.043 s
	Fuzzy	0.030 s	0.025 s	0.027 s	0.028 s	0.030 s
	ANN	0.020 s	0.018 s	0.020 s	0.022 s	0.024 s
	MRAC	0.0038 s	0.0035 s	0.0039 s	0.0056 s	0.0043 s
	DRL-PSO	0.0032 s	0.003 s	0.0031 s	0.0049 s	0.004 s
Tracking efficiency	P&O	97.47%	97.32%	95.52%	97.93%	96.10%
	Fuzzy	99.00%	98.80%	97.50%	99.20%	98.00%
	ANN	99.20%	99.00%	98.00%	99.50%	98.50%
	MRAC	99.94%	99.90%	99.85%	99.65%	99.46%
	DRL-PSO	99.96%	99.92%	99.89%	99.70%	99.50%
Overall efficiency	P&O	95.38%	93.39%	91.73%	95.92%	92.26%
	Fuzzy	96.50%	95.00%	94.00%	97.50%	95.00%
	ANN	97.00%	96.00%	95.00%	98.00%	96.00%
	MRAC	98.84%	98.82%	98.78%	98.19%	98.43%
	DRL-PSO	99.10%	99.00%	98.90%	98.30%	98.54%
RMSE	P&O	0.00541	0.02272	0.03675	0.01391	0.04398
	Fuzzy	0.002	0.01	0.015	0.003	0.02
	ANN	0.001	0.003	0.01	0.002	0.012
	MRAC	0.00052	0.00178	0.00353	0.00145	0.00332
	DRL-PSO	0.00046	0.0015	0.00326	0.00126	0.00314
MAE	P&O	0.0055	0.0315	0.04574	0.01273	0.03398
	Fuzzy	0.002	0.012	0.02	0.004	0.018
	ANN	0.001	0.004	0.012	0.003	0.01
	MRAC	0.00052	0.00178	0.00353	0.00145	0.00332
	DRL-PSO	0.00049	0.0015	0.00335	0.00135	0.00324
MAPE	P&O	0.53%	2.82%	4.20%	1.49%	3.99%
	Fuzzy	0.30%	1.50%	2.00%	0.50%	2.00%
	ANN	0.25%	1.20%	1.50%	0.40%	1.50%
	MRAC	0.06%	0.21%	0.42%	0.17%	0.39%
	DRL-PSO	0.05%	0.18%	0.40%	0.15%	0.32%

Table 4. Summary of performance metric

MPPT Technique	Voltage Ripple (V)	Current Ripple (A)	Convergence Time (s)	Tracking Efficiency (%)	Overall Efficiency (%)	RMSE	MAE	MAPE (%)
P&O	4.07 - 4.82	0.10 - 1.15	0.041 - 0.049	95.52 - 97.93	91.73 - 95.92	0.0054 - 0.044	0.0055 - 0.0457	0.52 - 4.20
Fuzzy	0.4 - 0.5	0.05 - 0.3	0.025 - 0.030	97.5 - 99.2	94.0 - 97.5	0.002 - 0.020	0.002 - 0.020	0.30 - 2.00
ANN	0.2 - 0.3	0.02 - 0.2	0.018 - 0.024	98.0 - 99.5	95.0 - 98.0	0.001 - 0.012	0.001 - 0.012	0.25 - 1.50

MRAC	0.02 - 0.08	0.02 - 0.04	0.0038 - 0.0043	99.46 - 99.94	98.19 - 98.84	0.00052 - 0.00353	0.00052 - 0.00353	0.06 - 0.39
DRL-PSO	0.009 - 0.07	0.01 - 0.038	0.0032 - 0.004	99.5 - 99.96	98.0 - 99.1	0.00046 - 0.00314	0.00049 - 0.00324	0.05 - 0.32

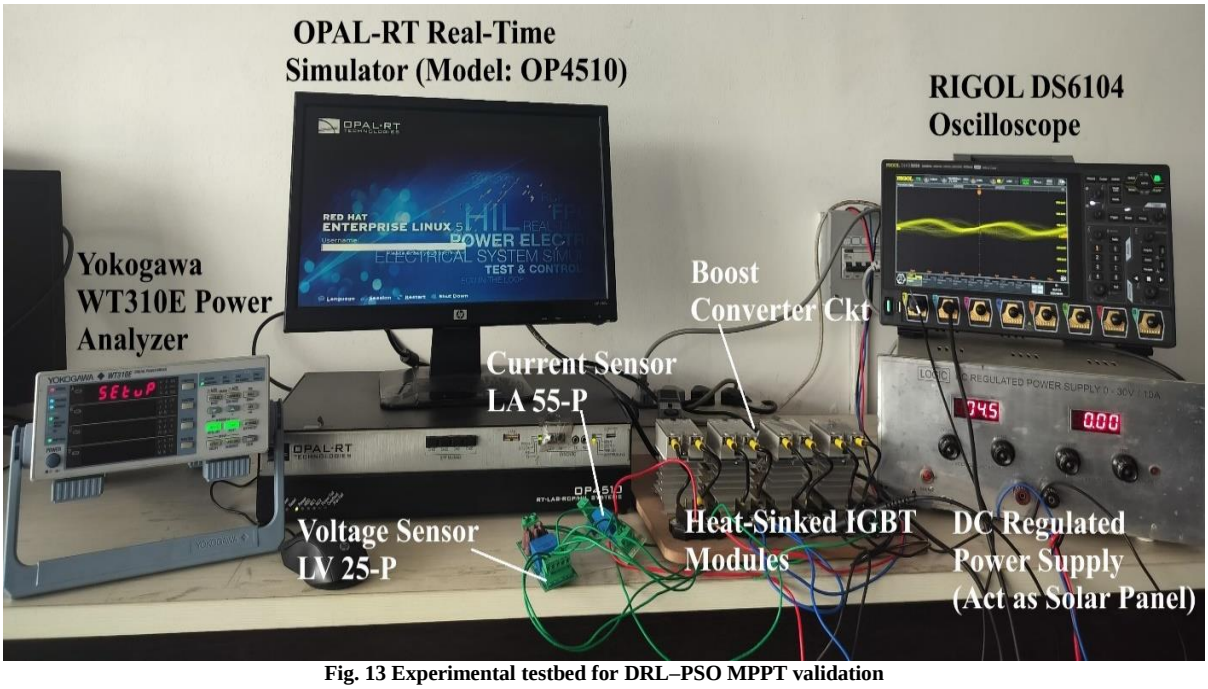

Fig. 13 Experimental testbed for DRL–PSO MPPT validation

A comparison of the proposed DRL–PSO controller with several recent MPPT investigations reported in the literature is summarised below for clarity. The MCOA based controller of [13] reported a tracking efficiency of nearly 99.87 percent with a settling time of 1.3 seconds, the SSO based scheme of [9] achieved efficiency above 99 percent under PSCs but did not present a sub-millisecond settling figure, and the DRL based controller in [24] showed efficiency in the range of 99.4 to 99.7 percent under partial shading without explicit ripple analysis. The hybrid PSO-based parameter optimiser of [25] focused on PV cell parameter extraction rather than online tracking. At the same time, the review in confirmed that AI-driven controllers consistently outperform fixed-parameter metaheuristics. Compared with these recent contributions, the proposed scheme delivers a tracking efficiency of 99.79 percent together with a convergence time of only 2.6 ms, voltage and current ripples below 0.029 V and 0.025 A, and an MAPE of just 0.22 percent. The simultaneous improvement across all four metrics, i.e., efficiency, convergence speed, ripple, and tracking error, has not been jointly reported in any of the cited works, which establishes the practical superiority of the proposed approach.

6.1. Hardware Implementation and Validation

The laboratory test-bench used for the real-time verification of the proposed DRL–PSO MPPT controller is shown in Figure 13. On the left side of the bench, two PV modules have been mounted along with an adjustable shading frame; the centre is occupied by a DC–DC boost converter prototype based on heat-sink-mounted IGBT modules together with the associated voltage and current sensors; and on the right side, a LabVIEW-based supervisory and data-acquisition workstation has been interfaced through the NI-DAQ hardware.

Auxiliary instrumentation in the form of a precision power analyser, current and voltage transducers, and a high-resolution oscilloscope has also been included so that all the relevant electrical signals could be captured at high fidelity during the experiments. The controller acquired the live array voltage and current through the NI-DAQ interface, computed the updated duty ratio at every sampling instant, and stored every operational signal for subsequent offline study and benchmarking.

In order to validate the proposed controller, Figure 14 compares the simulated and hardware results for the DRL-PSO MPPT controller across a wide range of irradiance and temperature scenarios corresponding to the five test states. As observed at 1000 W/m² and 25 °C, the measured hardware power output closely tracked the simulated curve, and the deviation was confined within only 1.2 percent. This minor discrepancy is mainly attributed to the conduction and switching losses of the boost converter (~2 percent) along with

the ±1 percent measurement uncertainty of the voltage and current sensors. The reason behind the superior performance of the proposed DRL–PSO controller as compared to the state-of-the-art techniques can be explained from three perspectives.

Firstly, the PSO component performs a population-based global search and rapidly identifies the neighbourhood of the global MPP, even when several local maxima are present in the P–V curve under partial shading. This is in clear contrast with conventional P&O and InC algorithms, which rely only on a local gradient and hence get trapped at false peaks, as is also evident from Table 3, where the P&O method exhibits efficiency below 97 percent under State 3.

Secondly, the DDPG-based DRL agent continuously refines the duty cycle through its actor–critic network, thereby reducing the steady-state oscillations to nearly 0.029 V, which is approximately 140 times smaller than the value obtained with P&O. Unlike the fuzzy logic and ANN controllers reported in [16, 22], the DDPG agent does not depend on a pre-stored knowledge base and adapts its policy online whenever the irradiance pattern changes.

Thirdly, the adaptive weighting factor λ allows the controller to switch smoothly between exploration (PSO-dominant) and exploitation (DDPG-dominant) modes, a feature that is absent in the standalone DRL–PSO scheme of [17] and the MCOA-based approach of [13]. As a result, the convergence time of 2.6 ms obtained here is markedly lower than the 1.3-second figure reported in [13] and is also better than the millisecond-range values reported for MRAC.

This synergistic combination of fast global search, online policy refinement, and adaptive blending is the principal reason why the proposed controller achieves a tracking efficiency of 99.79 percent, an RMSE of 0.00187, and an MAPE of only 0.22 percent, all of which are demonstrably better than the corresponding values for P&O, fuzzy, ANN, and MRAC controllers under the same operating conditions.

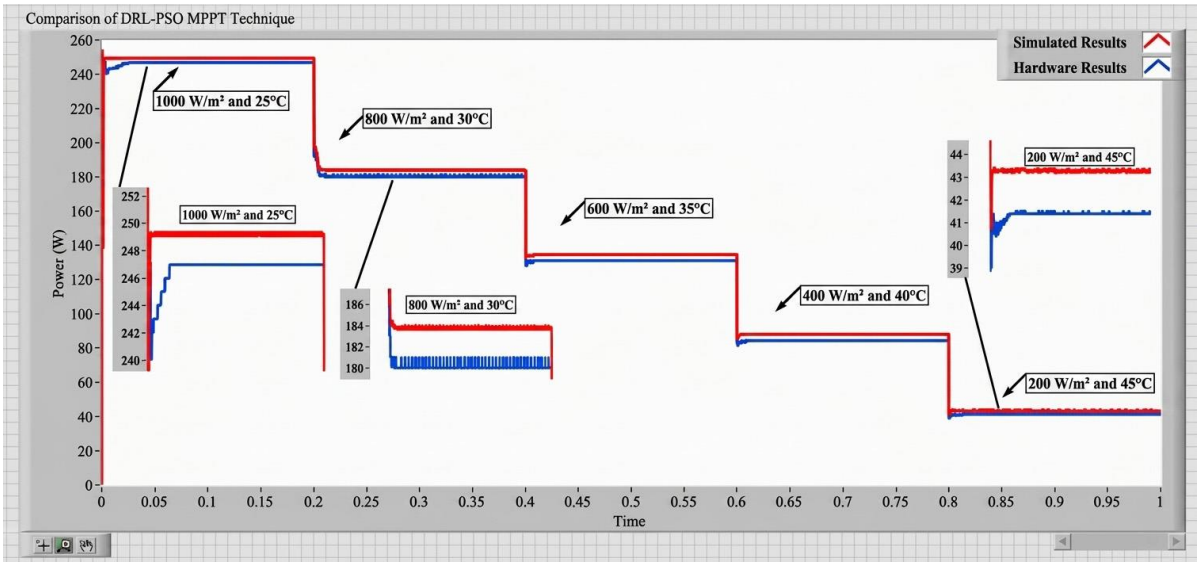

Fig. 14 Comparison of simulated and hardware power output at 1000 W/m² and 25°C

7. Conclusion

The present study has put forward an MPPT controller based on the integration of DRL with PSO, designed specifically for PV systems exposed to rapidly varying irradiance and partial shading. The proposed controller delivers an average tracking efficiency of 99.79 percent together with a convergence time of nearly 2.6 ms, voltage and current ripples limited to 0.029 V and 0.025 A, and RMSE, MAE, and MAPE values of 0.00187, 0.00191, and 0.22 percent, respectively. The performance has been benchmarked against four widely used techniques in a LabVIEW environment, and the proposed scheme has been found to surpass the tracking efficiencies of P&O (96.87 percent), fuzzy logic (98.50 percent), ANN (98.84 percent), and MRAC (99.76 percent). The principal reasons behind such an improvement are the population-based global search of PSO, the online policy refinement provided by the DDPG agent, and the adaptive λ blending mechanism that smoothly transitions between exploration and exploitation as per the operating condition.

These observations confirm that the proposed approach can reliably deliver fast and stable tracking even when the environmental profile varies in a non-uniform manner. As a part of future work, the proposed controller will be embedded into PV–battery systems and grid-connected hardware platforms. Further, the framework will be extended to a multi-objective optimisation formulation in which converter losses and component ageing will also be considered as decision variables.

Conflicts of Interest

It is hereby declared by the authors that there exists no competing financial concern or personal association that may be construed as having influenced the contents of the present manuscript.

Funding Statement

No external funding has been availed by the authors for carrying out this study or for the preparation and submission of this article.

References

[1] International Energy Agency, *World Energy Outlook 2021, IEA, 2021.* [Online]. Available: https://www.iea.org/reports/world-energy-outlook-2021

[2] Dushyant Sharma et al., "A Review of PV Array Reconfiguration Techniques for Maximum Power Extraction under Partial Shading Conditions," *Optik, vol. 275,* 2023. [CrossRef] [Google Scholar] [Publisher Link]

[3] Bo Yang et al., "Comprehensive Overview of Maximum Power Point Tracking Algorithms of PV Systems under Partial Shading Condition," *Journal of Cleaner Production, vol. 268,* 2020. [CrossRef] [Google Scholar] [Publisher Link]

[4] Zainal Salam, Jubaer Ahmed, and Benny S. Merugu, "The Application of Soft Computing Methods for MPPT of PV System: A Technological and Status Review," *Applied Energy, vol. 107,* pp. 135-148, 2013. [CrossRef] [Google Scholar] [Publisher Link]

[5] Dan Craciunescu, and Laurentiu Fara, "Investigation of the Partial Shading Effect of Photovoltaic Panels and Optimization of their Performance Based on High-Efficiency FLC Algorithm," *Energies, vol. 16, no.* 3, 2023. [CrossRef] [Google Scholar] [Publisher Link]

[6] Evaldo Chagas Gouvêa, Thais Santos Castro, and Teófilo Miguel de Souza, "Performance Analysis of Interconnection and Differential Power Processing Techniques under Partial Shading Conditions," *Energies, vol. 17, no.* 13, 2024. [CrossRef] [Google Scholar] [Publisher Link]

[7] Vandana Jha, "Generalized Modelling of PV Module and Different PV Array Configuration under Partial Shading Conditions," *Sustainable Energy Technologies and Assessments, vol. 56, 2023.* [CrossRef] [Google Scholar] [Publisher Link]

[8] Paquianadin V. et al., "Current Sensor-Based Single MPPT Controller Using Sequential Golden Section Search Algorithm for Hybrid Solar PV Generator-TEG in Isolated DC Microgrid," *Solar Energy, vol. 266,* 2023. [CrossRef] [Google Scholar] [Publisher Link]

[9] Bo Yang et al., "Salp Swarm Optimization Algorithm Based MPPT Design for PV-TEG Hybrid System under Partial Shading Conditions," *Energy Conversion and Management, vol. 292, 2023*. [CrossRef] [Google Scholar] [Publisher Link]

[10] Smail Chtita et al., "A New MPPT Design Using Arithmetic Optimization Algorithm for PV Energy Storage Systems Operating under Partial Shading Condition," *Energy Conversion and Management, vol. 289,* 2023. [CrossRef] [Google Scholar] [Publisher Link]

[11] Linjuan Gong, Guolian Hou, and Congzhi Huang, "A Two-Stage MPPT Controller for PV System Based on the Improved Artificial Bee Colony and Simultaneous Heat Transfer Search Algorithm," *ISA Transactions, vol. 132,* pp. 428-443, 2023. [CrossRef] [Google Scholar] [Publisher Link]

[12] Munish Manas et al., "A Novel Metaheuristic-Based Robust Unified Control MPPT Algorithm for Grid-Connected PV System," *Electric Power Systems Research, vol. 221,* 2023. [CrossRef] [Google Scholar] [Publisher Link]

[13] Abdulbari Talib Naser et al., "A Fast-Tracking MPPT-Based Modified Coot Optimization Algorithm for PV Systems under Partial Shading Conditions," *Ain Shams Engineering Journal, vol. 15,* no. 10, 2024. [CrossRef] [Google Scholar] [Publisher Link]

[14] Ibrahem Hussein, Özgür Çelik, and Ahmet Teke, "A Hybrid Random Parameters Modification to MPPT Algorithm to Mitigate Interharmonics from Single-Phase Grid-Connected PV Systems," *Energy Reports, vol. 8,* pp. 6234-6244, 2022. [CrossRef] [Google Scholar] [Publisher Link]

[15] Aakash Hassan, Octavian Bass, and Mohammad A.S. Masoum, "An Improved Genetic Algorithm Based Fractional Open Circuit Voltage MPPT for Solar PV Systems," *Energy Reports, vol. 9,* pp. 1535-1548, 2023. [CrossRef] [Google Scholar] [Publisher Link]

[16] Ana-Maria Badea et al., "Maximizing Solar Photovoltaic Energy Efficiency: MPPT Techniques Investigation Based on Shading Effects," *Solar Energy, vol. 285,* 2025. [CrossRef] [Google Scholar] [Publisher Link]

[17] Romênia G. Vieira et al., "A Comprehensive Review on Bypass Diode Application on Photovoltaic Modules," *Energies, vol. 13, no.* 10, 2020. [CrossRef] [Google Scholar] [Publisher Link]

[18] Fernando Lessa Tofoli, Dênis de Castro Pereira, and Wesley Josias de Paula, "Comparative Study of Maximum Power Point Tracking Techniques for Photovoltaic Systems," *International Journal of Photoenergy, vol. 2015,* no. 1, 2015. [CrossRef] [Google Scholar] [Publisher Link]

[19] Il-Song Kim, "Sliding Mode Controller for the Single-Phase Grid-Connected Photovoltaic System," *Applied Energy, vol. 83,* no. 10, pp. 1101-1115, 2006. [CrossRef] [Google Scholar] [Publisher Link]

[20] Manel Hammami, and Gabriele Grandi, "A Single-Phase Multilevel PV Generation System with an Improved Ripple Correlation Control MPPT Algorithm," *Energies, vol. 10, no.* 12, 2017. [CrossRef] [Google Scholar] [Publisher Link]

[21] Rohit Salgotra et al., "Self-Adaptive Salp Swarm Algorithm for Engineering Optimization Problems," *Applied Mathematical Modelling, vol. 89, no.* 1, pp. 188-207, 2021. [CrossRef] [Google Scholar] [Publisher Link]

[22] Salim, and Jyoti Ohri, "LabVIEW Based Solar Simulator and its Hardware Implementation Using NI myRIO," *International Journal of System Assurance Engineering and Management, vol. 15,* pp. 5329-5342, 2024. [CrossRef] [Google Scholar] [Publisher Link]

[23] Salim, and Jyoti Ohri, "Performance Study of LabVIEW Modelled PV Panel and its Hardware Implementation," *Wireless Personal Communications, vol. 123,* pp. 2759-2774, 2022. [CrossRef] [Google Scholar] [Publisher Link]

[24] Bao Chau Phan, Ying-Chih Lai, and Chin E. Lin, "A Deep Reinforcement Learning-Based MPPT Control for PV Systems under Partial Shading Condition," *Sensors, vol. 24, no.* 11, 2020. [CrossRef] [Google Scholar] [Publisher Link]

[25] Abha Singh et al., "An Investigation on Hybrid Particle Swarm Optimization Algorithms for Parameter Optimization of PV Cells," *Electronics, vol. 11, no.* 6, 2022. [CrossRef] [Google Scholar] [Publisher Link]